Monthly Notices
of the
ROYAL ASTRONOMICAL SOCIETY

MNRAS **459,** L61–L65 (2016)
Advance Access publication 2016 March 28

doi:10.1093/mnrasl/slw053

Discovery of a loose star cluster in the Large Magellanic Cloud

Andrés E. Piatti[1,2]★

[1]*Observatorio Astronómico, Universidad Nacional de Córdoba, Laprida 854, 5000 Córdoba, Argentina*
[2]*Consejo Nacional de Investigaciones Científicas y Técnicas, Av. Rivadavia 1917, C1033AAJ Buenos Aires, Argentina*

Accepted 2016 March 21. Received 2016 March 15; in original form 2016 February 16

ABSTRACT

We present results for an up-to-date uncatalogued star cluster projected towards the Eastern side of the Large Magellanic Cloud (LMC) outer disc. The new object was discovered from a search of loose star cluster in the Magellanic Clouds' (MCs) outskirts using kernel density estimators on Washington CT_1 deep images. Contrarily to what would be commonly expected, the star cluster resulted to be a young object ($\log(t\,\mathrm{yr}^{-1}) = 8.45$) with a slightly subsolar metal content ($Z = 0.013$) and a total mass of $650\,\mathrm{M}_{\odot}$. Its core, half-mass and tidal radii also are within the frequent values of LMC star clusters. However, the new star cluster is placed at the Small Magellanic Cloud distance and at 11.3 kpc from the LMC centre. We speculate with the possibility that it was born in the inner body of the LMC and soon after expelled into the intergalactic space during the recent Milky Way/MCs interaction. Nevertheless, radial velocity and chemical abundance measurements are needed to further understand its origin, as well as extensive search for loose star clusters in order to constrain the effectiveness of star cluster scattering during galaxy interactions.

Key words: techniques: photometric – galaxies: individual: LMC – Magellanic Clouds.

1 INTRODUCTION

Star clusters in the outer disc of the Large Magellanic Cloud (LMC; beyond $\sim 4^{\circ}$ from its centre; Bica et al. 1998) have long caught the astronomers' interest because of the common thought that they could be old and hence, it would be feasible from them to reconstruct the early galaxy formation and chemical enrichment history. Indeed, the spatial distribution of the studied star clusters shows that the outer disc is mainly populated by those of intermediate-age ($\gtrsim$2 Gyr) and old ones as well, in contrast with the much more numerous and younger star clusters that populate the inner disc (Glatt, Grebel & Koch 2010; Piatti et al. 2009). From a chemical evolution point of view, the outer disc is commonly featured as a more metal-poor structure ([Fe/H] $\lesssim -0.5$ dex) than the inner LMC body (Harris & Zaritsky 2009; Meschin et al. 2014).

Recently, a network of streams surrounding the LMC have been discovered (see e.g. Belokurov & Koposov 2016). They could be ram-pressure tails and relics of the collision between both Magellanic Clouds (MCs) (Hammer et al. 2015; Salem et al. 2015) and hence they could contain young star clusters. Indeed, the Magellanic Bridge harbours very young and intermediate-age star clusters as a result of the *in situ* star formation and stripping from tidal interaction between both galaxies (Bica et al. 2015).

In this Letter we introduce a new star cluster, discovered towards the Eastern part of the LMC outer disc and located at the Small Magellanic Cloud (SMC) distance. Its relatively low surface brightness could make it undetectable by previous LMC star cluster cataloguing efforts. The new star cluster is unexpectedly a relatively young object with a slightly subsolar global metal content. In order to unveil its origin, we took into account all the star cluster properties derived here, and from them we speculate with the possibility of being first discovered star cluster that was born in the LMC and soon ejected into the intergalactic space during the recent Milky Way/MCs interaction (Kallivayalil et al. 2013; Casetti-Dinescu et al. 2014; Indu & Subramaniam 2015).

2 STAR CLUSTER DISCOVERY AND ITS FUNDAMENTAL PARAMETERS

We searched for loose star clusters in the outer regions of the L/SMC by using Washington CT_1 images obtained at the Cerro Tololo Inter-American Observatory 4-m Blanco telescope with the Mosaic II camera attached (a 8K×8K CCD detector array, 36×36 arcmin^2), which are available at the National Optical Astronomy Observatory (NOAO) Science Data Management Archives.[1] The images were reduced and the photometric catalogues produced by Piatti (2012), Piatti, Geisler & Mateluna (2012) and Piatti (2015), respectively. The 30 fields surveyed amounts a total area of $324^{\circ 2}$. The 50 per cent completeness level of the resulting photometry is located at a T_1

★E-mail: andres@oac.unc.edu.ar

[1] http://www.noao.edu/sdm/archives.php.

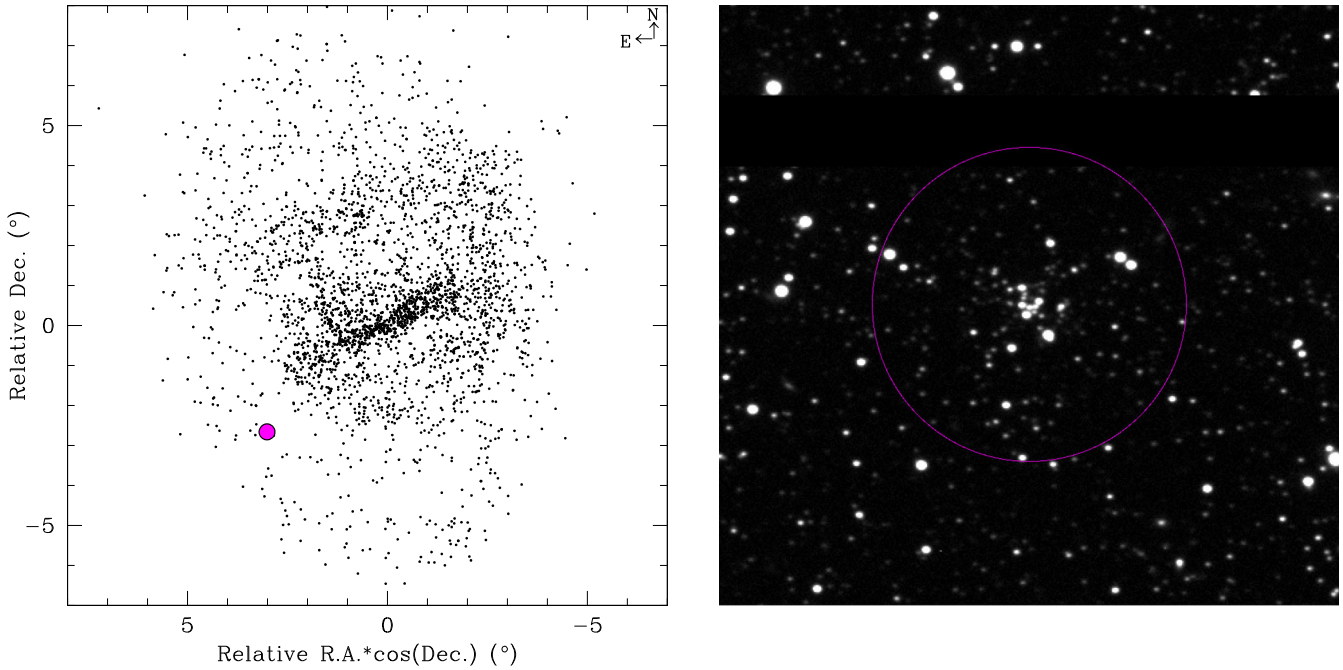

Figure 1. Left: spatial distribution of the Bica et al. (2008)'s catalogue of star clusters in the LMC centred at R.A. $= 05^{\rm h}23^{\rm m}34^{\rm s}$, Dec. $= -69^{\circ}45'22''$ (J2000), projected on to the sky. The discovered object is highlighted with a magenta-coloured filled circle. Right: A $1' \times 1'$ R image centred on the new LMC star cluster. North is up and East to the left. The star cluster radius is also superimposed.

Table 1. Properties of the new star cluster.

Parameter	Value
Equatorial coords.	$\alpha_{J2000} = 6^{\rm h}3^{\rm m}25.46^{\rm s}$
	$\delta_{J2000} = -72^{\circ}24'54.11''$
Galactc coords.	$l = 283.108^{\circ}$
	b $= -29.3795^{\circ}$
Distance modulus	$(m-M)_o = 18.90 \pm 0.05$ mag
Distance	$d = 60.3 \pm 1.4$ kpc
Reddening	$E(B-V) = 0.08 \pm 0.01$ mag
log(Age)	$\log(t\ {\rm yr}^{-1}) = 8.45 \pm 0.05$
Age	$t = 280^{+35}_{-30}$ Myr
Metallicity	[Fe/H] $= -0.10 \pm 0.05$ dex
Total mass	$M = 650 \pm 100$ M$_{\odot}$
Radius	$r = 9.23 \pm 2.69$ pc
Core radius	$r_c = 2.76 \pm 0.39$ pc
Half-mass radius	$r_h = 5.33 \pm 0.51$ pc
Tidal radius	$r_t = 19.72 \pm 3.94$ pc
Jacobi radius	$r_j = 13.5 \pm 2.3$ pc

magnitude and a $C - T_1$ colour corresponding to the main sequence (MS) turnoff of a stellar population with an age $\gtrsim$10 Gyr.

The search was performed by employing AstroML routines (Vanderplas et al. 2012, and reference therein for a detail description of the complete AstroML package and user's Manual), a machine learning and data mining for Astronomy package. We used two different kernel density estimators, namely, *Gaussian* and *tophat*, and bandwidths from 0.2 up to 1.0 arcmin for each L/SMC field photometric catalogue with stars measured in the two CT_1 filters. From the total number of stellar overdensities detected per field, we imposed a cut off density of 3σ above the background level and merged the resulting lists, avoiding repeated findings from different runs with different bandwidths. We finally identified one new star cluster from the L/SMC fields surveyed (see Fig. 1). Its central coordinates are listed in Table 1.

We built the star cluster density profile based on completeness corrected star counts previously performed within boxes of 5 up to 30 pixels a side distributed throughout the whole field of the star cluster. The selected size range of the boxes allowed us to sample statistically the stellar spatial distribution. Thus, the number of stars per unit area at a given radius, r, can be directly calculated through the expression:

$$(n_{r+} - n_{r-b/2})/(m_{r+b/2} - m_{r-b/2}), \quad (1)$$

where n_j and m_j represent the number of stars and boxes included in a circle of radius j, and b the box size, respectively. Note that this method does not necessarily require a complete circle of radius r within the observed field to estimate the mean stellar density at that distance. We used equation (1) because of the horizontal image gap (see Fig. 1) and the need of having a stellar density profile which extends far away from the star cluster centre to estimate the background level with high precision. This is necessary to derive the cluster radius (see Table 1). The resulting mean density profile is shown in Fig. 2 (bottom-right panel). In the figure, we represent the constructed and background subtracted density profiles with open and filled circles, respectively. Errorbars represent rms errors, to which we added the mean error of the background star count to the background subtracted density profile. The background level and the cluster radius are indicated by solid horizontal and vertical lines, respectively; their uncertainties are in dotted lines.

The background corrected density profile was fitted using a King (1962)'s model through the expression:

$$N \propto \left(\frac{1}{\sqrt{1+(r/r_c)^2}} - \frac{1}{\sqrt{1+(r_t/r_c)^2}} \right)^2 \quad (2)$$

where r_c and r_t are the core and tidal radii, respectively (see Table 1 and Fig. 2). As can be seen, the King profile satisfactorily reproduces the whole cluster extension. Nevertheless, in order

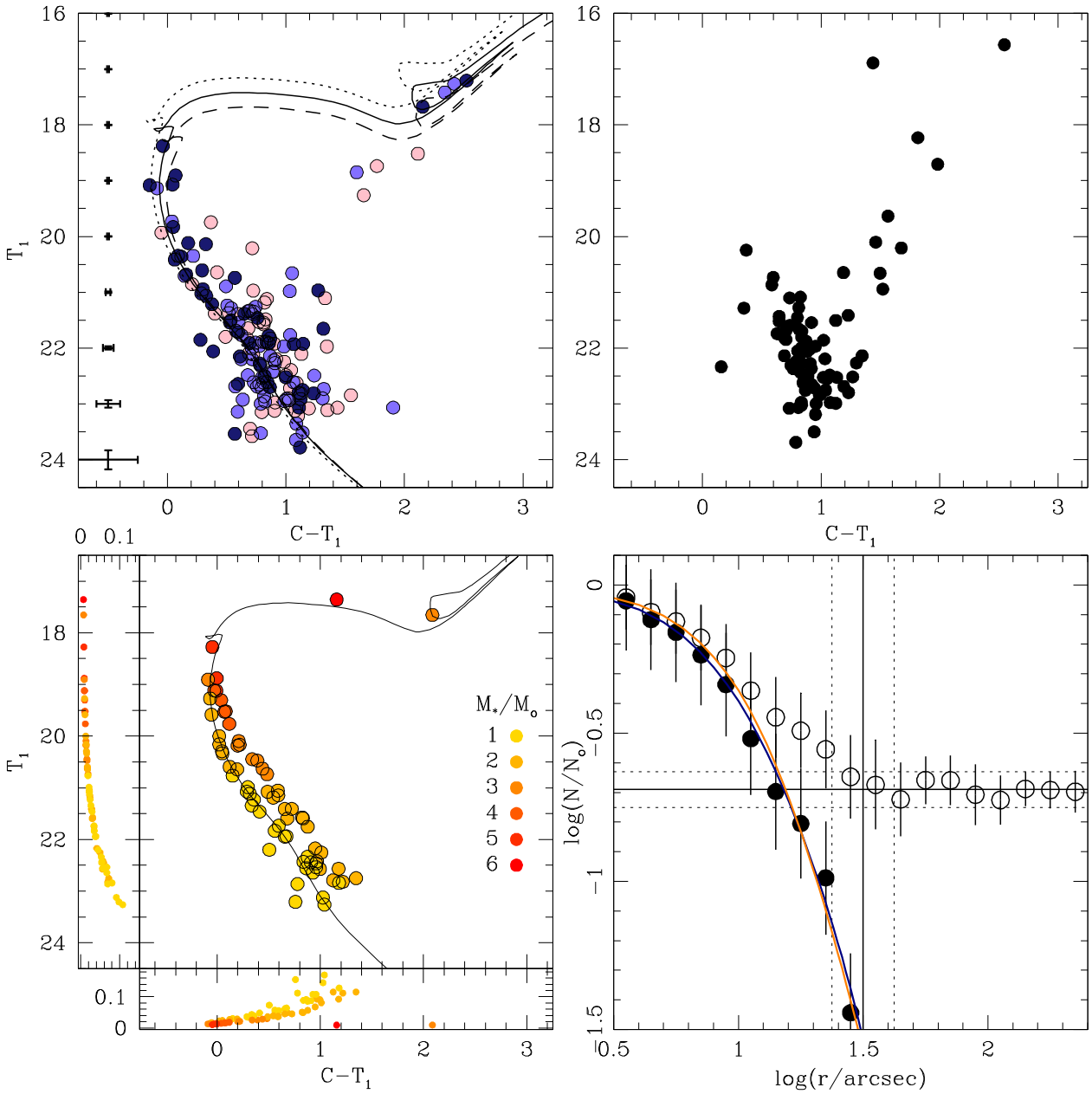

Figure 2. Top-left: the cleaned star cluster CMD. Colour-scaled symbols represent stars that statistically belong to the field ($P \leq 25$ per cent, pink), stars that might belong to either the field or the cluster ($P = 50$ per cent, light blue), and stars that predominantly populate the cluster region ($P \geq 75$ per cent, dark blue). Three isochrones from Bressan et al. (2012) for log(t yr^{-1}) = 8.40 ($Z = 0.011$), 8.45 ($Z = 0.013$) and 8.50 ($Z = 0.014$) are also superimposed (see the text for details). Top-right: a star field CMD for an annulus – outer and inner radii equal to 2.23 and 2.0 times the star cluster radius – centred on the star cluster. Bottom-left: best-generated star cluster CMD with the uncertainties in T_1 and $C - T_1$, the stellar masses in colour-scaled filled circles, and the best-fitted theoretical isochrone superimposed. Bottom-right: density profile obtained from star counts. Open and filled circles refer to measured and background subtracted density profiles, respectively. Blue and orange solid lines depict the fitted King and Plummer curves, respectively.

to get independent estimates of the star cluster half-mass radius, we fitted a Plummer's profile using the expression:

$$N \propto \frac{1}{(1 + (r/a)^2)^2} \quad (3)$$

where a is the Plummer's radius, which is related to the half-mass radius (r_h) by the relation $r_h \sim 1.3a$ (see Table 1 and Fig. 2).

In order to clean the star cluster colour–magnitude diagram (CMD) from the unavoidable field star contamination we applied a procedure developed by Piatti & Bica (2012). In short, the star field cleaning relies on the comparison of each of four previously defined field CMDs to the cluster CMD and subtracted from the latter a representative field CMD in terms of stellar density, luminosity function, and colour distribution. This was done by comparing the numbers of stars counted in boxes distributed in a similar manner throughout all CMDs. The boxes were allowed to vary in size and position throughout the CMDs in order to meaningfully represent the actual distribution of field stars. Since we repeated this task for each of the four field CMDs, we could assign a membership probability to each star in the cluster CMD. This was done by counting

the number of times a star remained unsubtracted in the four cleaned cluster CMDs and by subsequently dividing this number by 4. Thus, we distinguished field populations projected on to the star cluster area, i.e. those stars with a probability $P \leq 25$ per cent, stars that could equally likely be associated with either the field or the object of interest ($P = 50$ per cent), and stars that are predominantly found in the cleaned star cluster CMDs ($P \geq 75$ per cent) rather than in the field star CMDs. We employed this field star decontamination procedure to clean a circular area of radius three times that of the star cluster around its central coordinates. Fig. 2 (top-left panel) shows the resulting cleaned CMD for stars located within the star cluster radius. As can be seen, the distribution of stars with $P \geq 75$ per cent resembles that of a relatively young star cluster. For comparison purposes we show in the top-right panel a field star CMD using an area placed in a ring with outer and inner radii of 2.23 and 2.0 times the star cluster radius.

In order to derive star cluster' astrophysical properties, we employed the `ASteCA` suit of functions (Perren, Vázquez & Piatti 2015) to generate synthetic CMDs of star clusters covering ages from $\log(t\,\mathrm{yr}^{-1}) = 8.0$ up to 9.0 ($\Delta\log(t\,\mathrm{yr}^{-1}) = 0.05$), metallicities in the range $Z = 0.003 - 0.025$ ($\Delta Z = 0.001$), interstellar extinction between 0.0 and 0.3 mag ($\Delta E(B-V) = 0.01$ mag), distance modulus between 18.0 and 19.5 mag ($\Delta(m-M)_o = 0.05$ mag) and total mass in the range 100–1000 $\mathrm{M}_\odot$ ($\Delta M = 50\,\mathrm{M}_\odot$), respectively. In total, we used $\approx 8.8 \times 10^6$ models.

The steps by which a synthetic star cluster for a given set of age, metallicity, distance modulus, and reddening values is generated by `ASteCA` is as follows: (i) a theoretical isochrone is picked up, densely interpolated to contain a thousand points throughout its entire length, including the most evolved stellar phases. (ii) The isochrone is shifted in colour and magnitude according to the $E(B-V)$ and $(m-M)_o$ values to emulate the effects these extrinsic parameters have over the isochrone in the CMD. (iii) The isochrone is trimmed down to a certain faintest magnitude according to the limiting magnitude thought to be reached. (iv) An initial mass function (IMF) is sampled in the mass range [∼0.01–100] $\mathrm{M}_\odot$ up to a total mass value M provided that ensures the evolved CMD regions result properly populated. The distribution of masses is then used to obtain a properly populated synthetic star cluster by keeping one star in the interpolated isochrone for each mass value in the distribution. (v) A random fraction of stars are assumed to be binaries, which is set by default to 50 per cent (von Hippel 2005), with secondary masses drawn from a uniform distribution between the mass of the primary star and a fraction of it given by a mass ratio parameter set to 0.7. (vi) An appropriate magnitude completeness and an exponential photometric error functions are finally applied to the synthetic star cluster.

As for our purposes, we used the theoretical isochrones computed by Bressan et al. (2012) using extensive tabulations of bolometric corrections with uncertainties ∼ 0.001 mag for the C and T_1 filters and the IMF of Kroupa (2002). Fig. 2 shows with a solid line the best-fitted theoretical isochrone to stars with $P \geq 50$ per cent, which corresponds to maximum likelihood values of: $E(B-V) = 0.08$ mag, $(m-M)_o = 18.9$ mag, $\log(t\,\mathrm{yr}^{-1}) = 8.45$ and $Z = 0.013$, respectively. In order to visually check the parameter dispersion, we bracketed that isochrone with two ones for the following parameter values: $E(B-V) = 0.07$ mag, $(m-M)_o = 18.85$ mag, $\log(t\,\mathrm{yr}^{-1}) = 8.40$ and $Z = 0.011$ (dotted line), and $E(B-V) = 0.08$ mag, $(m-M)_o = 18.95$ mag, $\log(t\,\mathrm{yr}^{-1}) = 8.50$ and $Z = 0.014$ (short-dashed line), respectively. The best synthetic star cluster CMD is depicted in the bottom-left panel of the figure, with the generated uncertainties in T_1 and $C - T_1$, the range of stellar masses drawn in colour-scaled filled circles and the best-fitted theoretical isochrones superimposed. The resulting mean values and errors for the different star cluster's properties are listed in Table 1.

From the derived mass we estimated both the Jacobi tidal radius and the half-mass relaxion time of the star cluster. The former was computed from the expression (Chernoff & Weinberg 1990):

$$r_J = \left(\frac{M_{\rm cls}}{3M_{\rm gal}}\right)^{1/3} \times d_{\rm GC} \qquad (4)$$

where $M_{\rm cls}$ is the total star cluster mass, $M_{\rm gal}$ is the LMC mass inside 8.7 kpc ($(1.7 \pm 0.7) \times 10^{10}$ $\mathrm{M}_\odot$,van der Marel & Kallivayalil (2014)), and $d_{\rm GC}$ is the star cluster deprojected galactocentric distance (4.532°). The resulting Jacobi radius compares well within the errors with the star cluster tidal radius, which suggests that the star cluster is not tidally truncated, i.e. it is not limited. This means that the star cluster is not expected to have lost significant amounts of stellar mass, so that its current mass should reflect its initial mass. Additionally, we found a half-mass density of 1.0 $\mathrm{M}_\odot$ pc^3. This value is much larger than the minimum density a star cluster needs to have in order to be stable against the tidal disruption of a galaxy (∼ $0.1\mathrm{M}_\odot$ pc^3, Bok (1934)). Accordingly, Wilkinson et al. (2003) also showed that the tidal field of the LMC does not cause any perturbation on the clusters.

On the other hand, for the half-mass relaxation times we used the equation (Spitzer & Hart 1971):

$$t_r = \frac{8.9 \times 10^5 M_{cls}^{1/2} r_h^{3/2}}{\bar{m} log_{10}(0.4 M_{cls}/\bar{m})}, \qquad (5)$$

where $M_{\rm cls}$ is the cluster mass, $r_{\rm h}$ is the half-mass radius and $\bar{m}$ is the average mass of the star cluster stars ($2.6 \pm 1.2\,\mathrm{M}_\odot$ from the generated synthetic CMD). The derived relaxation time resulted to be $t_{\rm r} = 53 \pm 15$ Myr.

3 DISCUSSION AND CONCLUSION

The derived $E(B-V)$ colour excess is in excellent agreement with the values obtained from both Haschke, Grebel & Duffau (2011, 0.06 mag) and Schlafly & Finkbeiner (2011, 0.09 mag) extinction maps, respectively, so that we infer that the star cluster is neither projected behind of, nor embedded into dense clouds of gas and dust. The star cluster is located at a distance of 60.3 kpc from the Sun, 11.3 kpc from the LMC centre and at a LMC angular distance of 4.532° East. Its spatial position and low reddening suggest that there is no dense streams behind the LMC in the star cluster line-of-sight, although streams have recently appeared to be more common around the LMC (Hammer et al. 2015; Salem et al. 2015). If our derived star cluster distance were wrong, i.e. the object should belong to the LMC disc according to its projected position in the sky, then it would be expected to have an age similar to those star clusters belonging to the outer LMC disc. However, three star clusters with age estimate, out of five star clusters located within a radius of 0.75° in the sky around the new star cluster are much older, $\log(t\,\mathrm{yr}^{-1}) = 9.25$, which is the age associated to the LMC outer disc (Piatti et al. 2009).

The derived age and metallicity agrees well with the global age–metallicity relationship (AMR) obtained by Piatti & Geisler (2013, see their fig. 6) for field stars and star clusters, respectively. The AMR of the SMC – considering either field stars or star clusters – follows a clearer different trend. It is in general ∼ 0.4 dex more metal-poor in [Fe/H] than that of the LMC (Piatti 2011; Piatti et al. 2015). This could imply that the new star cluster hardly possible was born in the SMC (present star cluster-SMC distance of 26.4 kpc) and

then stripped by the LMC. It would be less conflicted to speculate with the possibility that it has been born in the LMC. Indeed, besides having an age and a metallicity compatible with the LMC AMR, there is also a good agreement for its age and mass with the age versus mass relationship shown by Baumgardt et al. (2013). In addition, its structural parameters (r_c, r, r_t) are all within the frequent values found for LMC star clusters (Werchan & Zaritsky 2011).

An unavoidable question arises: how to explain the presence of a star cluster located at the SMC distance from the Sun and 26.4 kpc far away from the SMC centre with astrophysical properties (metallicity, mass, structural parameters) which resemble those of relatively young LMC star clusters? We think that the star cluster could have recently been ejected from the LMC inner body as a consequence of tidal interaction with the Milky Way/SMC. Indeed, close Milky Way/SM passages have been predicted from computation of their orbital motions (Kallivayalil et al. 2013). Nevertheless, spectroscopic observations for radial velocity and chemical abundance measurements are needed to further understand its origin. Furthermore, in order to constrain the effectiveness of star cluster scattering during galaxy interaction, it would be worth to search for additional star clusters from, for instance, the DECam survey of the MCs (Nidever et al. 2013).

ACKNOWLEDGEMENTS

We thank the anonymous referee whose comments and suggestions allowed us to improve the manuscript.

REFERENCES

Baumgardt H., Parmentier G., Anders P., Grebel E. K., 2013, MNRAS, 430, 676
Belokurov V., Koposov S. E., 2016, MNRAS, 456, 602
Bica E., Bonatto C., Dutra C. M., Santo J. F. C., 2008, MNRAS, 389, 678
Bica E., Geisler D., Dottori H., Clariá J. J., Piatti A. E., Santos J. F. C., Jr, 1998, AJ, 116, 723
Bica E., Santiago B., Bonatto C., Garcia-Dias R., Kerber L., Dias B., Barbuy B., Balbinot E., 2015, MNRAS, 453, 3190
Bok B. J., 1934, Harv. Coll. Obs. Circ., 384, 1
Bressan A., Marigo P., Girardi L., Salasnich B., Dal Cero C., Rubele S., Nanni A., 2012, MNRAS, 427, 127
Casetti-Dinescu D. I., Moni Bidin C., Girard T. M., Méndez R. A., Vieira K., Korchagin V. I., van Altena W. F., 2014, ApJ, 784, L37
Chernoff D. F., Weinberg M. D., 1990, ApJ, 351, 121
Glatt K., Grebel E. K., Koch A., 2010, A&A, 517, A50
Hammer F., Yang Y. B., Flores H., Puech M., Fouquet S., 2015, ApJ, 813, 110
Harris J., Zaritsky D., 2009, AJ, 138, 1243
Haschke R., Grebel E. K., Duffau S., 2011, AJ, 141, 158
Indu G., Subramaniam A., 2015, A&A, 573, A136
Kallivayalil N., van der Marel R. P., Besla G., Anderson J., Alcock C., 2013, ApJ, 764, 161
King I., 1962, AJ, 67, 471
Kroupa P., 2002, Science, 295, 82
Meschin I., Gallart C., Aparicio A., Hidalgo S. L., Monelli M., Stetson P. B., Carrera R., 2014, MNRAS, 438, 1067
Nidever D. et al., 2013, Survey of the MAgellanic Stellar History – SMASH, NOAO Proposal
Perren G. I., Vázquez R. A., Piatti A. E., 2015, A&A, 576, A6
Piatti A. E., 2011, MNRAS, 418, L69
Piatti A. E., 2012, MNRAS, 422, 1109
Piatti A. E., 2015, MNRAS, 451, 3219
Piatti A. E., Bica E., 2012, MNRAS, 425, 3085
Piatti A. E., Geisler D., 2013, AJ, 145, 17
Piatti A. E., Geisler D., Sarajedini A., Gallart C., 2009, A&A, 501, 585
Piatti A. E., Geisler D., Mateluna R., 2012, AJ, 144, 100
Piatti A. E., de Grijs R., Rubele S., Cioni M.-R. L., Ripepi V., Kerber L., 2015, MNRAS, 450, 552
Salem M., Besla G., Bryan G., Putman M., van der Marel R. P., Tonnesen S., 2015, ApJ, 815, 77
Schlafly E. F., Finkbeiner D. P., 2011, ApJ, 737, 103
Spitzer L., Jr, Hart M. H., 1971, ApJ, 164, 399
van der Marel R. P., Kallivayalil N., 2014, ApJ, 781, 121
Vanderplas J., Connolly A., Ivezić Ž., Gray A., 2012, in Kamalika D., Nitesh V. C., Ashok N. S., eds, Conference on Intelligent Data Understanding (CIDU), Introduction to astroML: Machine Learning for Astrophysics. Institute of Electrical and Electronics Engineers (IEEE) Conference Publications, USA, p. 47
von Hippel T., 2005, ApJ, 622, 565
Werchan F., Zaritsky D., 2011, AJ, 142, 48
Wilkinson M. I., Hurley J. R., Mackey A. D., Gilmore G. F., Tout C. A., 2003, MNRAS, 343, 1025

This paper has been typeset from a TEX/LATEX file prepared by the author.